



## Imaging the sources and full extent of the sodium tail of the planet Mercury

Jeffrey Baumgardner,<sup>1</sup> Jody Wilson,<sup>1</sup> and Michael Mendillo<sup>1</sup>

Received 15 October 2007; revised 19 November 2007; accepted 5 December 2007; published 2 February 2008.

[1] Observations of sodium emission from Mercury can be used to describe the spatial and temporal patterns of sources and sinks in the planet's surface-boundary-exosphere. We report on new data sets that provide the highest spatial resolution of source regions at polar latitudes, as well as the extraordinary length of a tail of escaping Na atoms. The tail's extent of  $\sim 1.5$  degrees (nearly 1400 Mercury radii) is driven by radiation pressure effects upon Na atoms sputtered from the surface in the previous  $\sim 15$  hours. Wide-angle filtered-imaging instruments are thus capable of studying the time history of sputtering processes of sodium and other species at Mercury from ground-based observatories in concert with upcoming satellite missions to the planet. Plasma tails produced by photo-ionization of Na and other gases in Mercury's neutral tails may be observable by in-situ instruments. **Citation:** Baumgardner, J., J. Wilson, and M. Mendillo (2008), Imaging the sources and full extent of the sodium tail of the planet Mercury, *Geophys. Res. Lett.*, 35, L03201, doi:10.1029/2007GL032337.

### 1. Introduction

[2] It has been known for more than 20 years [Potter and Morgan, 1985] that the planet Mercury is a source of neutral sodium atoms. The light scattered from these atoms at 589.0 nm and 589.6 nm has been detected spectroscopically and mapped across the planet's disk [e.g., Sprague *et al.*, 1997; Barbieri *et al.*, 2004; Leblanc *et al.*, 2006], depicted directly in two dimensions by the use of a spectrographic image slicer [e.g., Potter and Morgan, 1997], as well as image slicers equipped with image stabilizers [Potter *et al.*, 2006]. Fabry-Perot imaging techniques have been applied to Mercury as well [Kameda *et al.*, 2007]. To our knowledge no 2-dimensional images have been published that were taken directly by cameras equipped with narrow band interference filters.

[3] Making spatially resolved maps of the sodium distribution on and near the disk of Mercury is a challenge, since typically the target has a small (between 5 and 12 arc-sec) angular diameter and it is usually observed at low elevation angles ( $< 15$  deg.) where the astronomical seeing is poor. Nevertheless, several groups of observers have produced images showing the sodium emission on and near Mercury's disk (e.g., as summarized in Figure 6.4 of Strom and Sprague [2003]). Interpretation of these sodium maps is difficult without detailed modeling of the motion of the sodium atoms and the use of sophisticated radiative transfer

codes, as the peak number density of the sodium atoms can be high enough to produce patches of optically thick atmosphere [Sprague *et al.*, 1997]. Even without considering the optical thickness issue, the derivation of the column abundance of atoms from the observed brightness is complicated by the fact that each sodium atom in the column "sees" a different solar flux depending on its radial speed and distance relative to the Sun.

[4] Sodium atoms have a high "g" factor for scattering photons at the D1 (589.6 nm) and D2 (589.0 nm) spectral lines [Chamberlain and Hunten, 1987]. For sodium atoms with near zero radial velocity relative to the Sun, the solar Fraunhofer lines at D1 and D2 reduce the flux available for this scattering to  $\sim 5\%$  of the solar continuum, as is the case when Mercury is near perihelion or aphelion. However, when the planet is  $\pm 16$  days from perihelion, this radial velocity approaches  $\pm 10$  km/sec, with a corresponding increase of the solar flux to  $\sim 45\%$  of the solar continuum, and produces a factor of  $\sim 10$  increase in the brightness of the sodium emission for a given column abundance. In addition to enhanced brightness due to Doppler shifts from the depth of the Fraunhofer absorption, the enhanced photon flux causes dramatic increases in the solar radiation acceleration imparted to the Na atoms. This feedback effect was realized soon after the discovery of sodium at Mercury, and was described in models by Ip [1986], Smyth [1986], and later in greater detail by Smyth and Marconi [1995] and observationally by Potter *et al.* [2007]. This paper deals with the extraordinary consequences of this effect at Mercury.

### 2. Sodium Tails

[5] Sodium tails have been observed streaming away from a number of solar system objects: comets [Combi *et al.*, 1997; Cremonese *et al.*, 1997; Wilson *et al.*, 1998], the Earth's Moon [Mendillo *et al.*, 1991; Smith *et al.*, 1999; Wilson *et al.*, 1999; Mierkiewicz *et al.*, 2006]; and Mercury [Potter *et al.*, 2002]. Each time a sodium atom scatters a solar photon, it recoils in the anti-sunward direction. At 1 A.U., a sodium atom at rest relative to the Sun experiences an acceleration of  $\sim 2.5$  cm/sec<sup>2</sup>. For atoms in highly eccentric trajectories above the Moon, for example, this acceleration is sufficient to strip some of these atoms from the Moon's gravity field and start them on their way down the tail. The discovery image of the lunar Na tail showed it to decrease from a few hundred Rayleighs (R) near the limb to  $\sim 5$  R at a distance of  $16 R_{\text{Moon}}$  [Mendillo *et al.*, 1991]. As these atoms accelerate away from the Sun, they move out of the Fraunhofer absorption line, experience increasing solar flux, and consequently an ever increasing acceleration. After  $\sim 50$  hours the atoms are moving at  $\sim 10$  km/

<sup>1</sup>Center for Space Physics, Boston University, Boston, Massachusetts, USA.

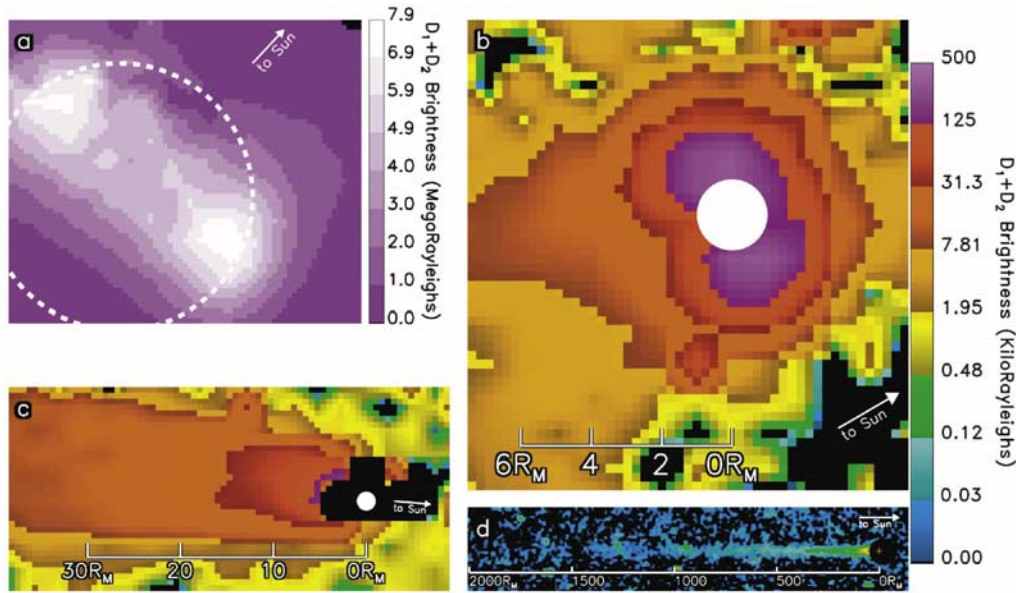


**Figure 1.** A composite of four images of sodium at Mercury showing spatial scales ranging from the diameter of the planet, to approximately 1000 times that size. Image obtained using (a) the 3.7 m AEOS telescope on Maui on June 8, 2006, and (b) the 0.4 m telescope at the Tohoku Observatory on Maui on June 10, 2006. (c, d) Obtained using the 0.4 m and 0.1 m telescopes at the Boston University Observing Station at the McDonald Observatory on the night of May 30, 2007. The images in Figures 1a, 1b, and 1c were obtained using a  $20 \times 20$  pixel image slicer, and 1d with a filtered coronagraph. Brightness calibrations were done using standard stars, with an overall uncertainty of  $\sim 20\%$ . The tail brightness levels at distances greater than  $\sim 10 R_M$  are greater in Figures 1c than 1b, and far greater than in work from *Potter et al.* [2002], a manifestation of exospheric variability.

sec. The time constant for Na to be ionized by solar UV radiation at 1 A.U. is  $\sim 47$  hrs [*Huebner et al.*, 1992; *Combi et al.*, 1997; *Cremonese et al.*, 1997], approximately the length of time for a sodium atom to travel the distance from the Moon to the Earth and beyond. For a few days around new moon phase, this lunar sodium tail can be imaged by ground-based observers as a small ( $\sim 5$  degree diameter) patch of emission near the anti-sunward direction [*Smith et al.*, 1999, 2001]. Fabry-Perot methods report down-tail velocities averaging 12.4 km/s near the center of this tail spot [*Mierkiewicz et al.*, 2006].

## 2.1. Sodium Tail Near Mercury

[6] Since modeling studies indicate that Mercury’s total neutral sodium production is perhaps  $\sim 100$  times the rate of the Moon [*Morgan and Killen*, 1997], coupled to the fact that the solar flux at Mercury’s average distance (and therefore the radiation pressure) is  $\sim 7$  times that at the Moon’s distance, while the surface gravity is only twice that of the Moon, it is expected that Mercury should have a sodium tail similar to that of the Moon, only brighter and longer. Indeed, the only observations to date of Na at Mercury spanning a broad spatial region [*Potter et al.*, 2002] showed brightness levels decreasing from  $\sim 6$  Mega-Rayleighs (MR) at the disk to  $\sim 600 R$  in a tail detected out to  $\sim 16$  Mercury radii ( $\sim 40,000$  km). Also, models of Mercury’s exosphere, from the earliest simulations of *Ip* [1986] and *Smyth* [1986], show sodium escaping to form a robust anti-sunward structure extending well beyond their simulation grids of several mercury radii. Given the often mentioned analogy between the exospheres

of the Moon and Mercury [*Morgan and Killen*, 1997; *Killen and Ip*, 1999; *Stern*, 1999; *Leblanc et al.*, 2007], observations of sodium using several fields of view are required to assemble datasets suitable for detailed simulation of source and escape processes at Mercury.

[7] In June 2006, as part of an International Mercury Watch (IMW) [*Mendillo and the IMW team*, 2007] a Boston University team made observations from Haleakela on Maui using two very different telescopes. Figure 1a is an image of Mercury’s sodium emission taken with the image-slicer spectrograph developed at Boston University [*Baumgardner et al.*, 2000]. The  $20 \times 20$  array of fibers was used to observe Mercury with the 3.7m AEOS telescope operated by the U.S. Air Force on Haleakela. Mercury’s diameter ( $\sim 6.5$  arc-sec) was near the upper limit where the AEOS adaptive optics system can provide correction for atmospheric seeing. The plate scale on the image slicer with this telescope is  $\sim 0.5$  arc-sec/fiber.

[8] The data in Figure 1a were taken on June 8, 2006, at a time when Mercury’s radial velocity was near the maximum value of 10 km/sec away from the Sun. Radiation acceleration on this date was  $\sim 170$  cm/s<sup>2</sup>, or nearly half of the surface gravity, producing substantial escape. As has been reported by other observers, the sodium emission is often not uniformly distributed over the surface of the planet but has “source spots” near the poles [e.g., *Potter et al.*, 2006; *Sprague et al.*, 1998] and a slight enhancement of emission near the morning terminator. Figure 1a is the highest resolution image of the polar sodium “patches” published to date. The origin of these high latitude sources is a matter of some debate [*Lammer et al.*, 2003; *Leblanc et al.*, 2007].

They could arise by the sputtering of energetic plasmas guided to the surface by Mercury's weak but global magnetic field [e.g., *Potter and Morgan*, 1990], or from the redistribution and accumulation at high latitudes of Na atoms liberated from the surface by thermal desorption or other processes [*Cremonese et al.*, 2005] and migrating night-ward in a series of ballistic hops [*Leblanc and Johnson*, 2003]. The important point is that these polar patches of sodium, while waxing and waning with time, are observed frequently and appear to be the dominant source regions for the higher velocity sputtered Na atoms that form the tail. This is not the case at the Moon where global (e.g., meteoritic) or hemispheric (solar/solar wind) sources are used to model its exosphere and tail. To see how Mercury's two high latitude source regions contribute to a tail requires a larger field of view.

[9] A few nights after the AEOS observations shown in Figure 1a, the imager slicer was moved to the focus of a 0.4 m telescope on Maui being operated by the IMW team from Tohoku University, in Sendai, Japan. The telescope was used at  $\sim f/30$ , yielding a plate scale of  $\sim 4$  arc-sec or 1 Mercury radius per fiber. Mercury's radial velocity at the time of this image was  $\sim 8$  km/s away from the sun. Figure 1b gives these results. The sodium atoms can be seen streaming back from the disk of Mercury, leaving the field of view in the anti-sunward direction, at  $\sim 12$  Mercury radii. Mercury's disk is just barely resolved in this image. Just as in the lunar case, this sodium tail has a core that is dimmer than its flanks. For the Moon, this is due to the Moon casting its shadow upon the sodium atoms in the tail, causing the tail to appear as a tube [*Mendillo et al.*, 1991]. This effect seems to be enhanced in the Mercury data, due to the concentrated sources at high latitudes. The magnitude of the shadow effect is approximately 60% (a lower limit considering that the disk of mercury is barely resolved in Figure 1b), considerably stronger than the 20–40% seen in the three datasets showing the same effect at the Moon [*Mendillo et al.*, 1991; *Flynn and Mendillo*, 1993].

[10] In May–June 2007, Mercury's sodium tail was imaged again with a 0.4 meter diameter telescope from the Boston University Station at the McDonald Observatory in Ft. Davis, Texas. The image slicer was used as before, but this time the telescope was operated at  $\sim f/10$  to increase the field of view and to increase the signal level at the image slicer input. As shown in Figure 1c, the tail can be seen leaving the field of view of the image slicer at  $\sim 30$  Mercury radii ( $\sim 70,000$  km). The tail width is also increasing over this distance due to a significant cross tail velocity component, as discussed by *Potter et al.* [2002]. The magnitude of this velocity is an indication of the lowest sputtering speed, typically  $\sim 2.0$  km/sec during maximum radiation acceleration [*Smyth and Marconi*, 1995], capable of being accelerated to Mercury's escape velocity (4.3 km/sec) by solar radiation pressure. As the sodium atoms continue to be accelerated down the tail, the apparent opening angle of the tail will get smaller, and the large-scale pattern will be a long, narrow parabola parallel to the direction of solar photons (to derive the magnitude of the original cross-tail velocity component from the observations detailed modeling has to be done, since the scattering of solar photons also can produce a cross-tail velocity component). The two lobe

nature of the tail seen on the 0.4 meter data from Maui (Figure 1b) is not evident in the McDonald data (Figure 1c), possibly due to the larger field of view used for the May 2007 data. The merging of the two tail lobes into a single tail, as shown in Figure 1c, points to the need for yet a larger field of view to map the full extent of the tail far from the planet.

## 2.2. Mercury's Distant Sodium Tail

[11] Most of the Boston University Mercury observing campaigns to date have been aimed at getting high resolution images of the surface [*Baumgardner et al.*, 2000] and the distribution (and possible variability) of sodium brightness on and near the disk. The fields of view used for these investigations are small ( $\sim 10$  to 45 arc-sec), a function of the focal length of the telescope used. The 0.4 meter diameter  $f/10$  telescope at the Boston University facility at the McDonald Observatory is routinely used with the image slicer and echelle spectrograph to monitor the Io plasma torus [*Wilson et al.*, 2005]. When in this configuration, the field of view of the image slicer is  $\sim 140$  arc-sec, with each fiber being approximately 7 arc-sec. This is the configuration that was used to take the data shown in Figure 1c. To see the total extent of the tail a much larger field of view is needed.

[12] A second, smaller (0.1 meter) aperture instrument is co-aligned with the 0.4 meter telescope at McDonald. This instrument was developed to study the extended sodium nebula surrounding Jupiter and to study the sodium exosphere of the Moon. To block the bright images of the Moon and Jupiter the instrument is configured as a coronagraph, so that long ( $\sim 2$  minute) exposures can be made without saturating the CCD. This instrument uses narrow-band ( $\sim 14$  Å HPFW) interference filters and images an 8 degree field of view at  $f/1.5$  onto a  $1024 \times 1024$  CCD, usually binned  $2 \times 2$  to  $512 \times 512$  pixels.

[13] During the May–June 2007 campaign at McDonald, this instrument was pointed at Mercury under excellent sky conditions when the planet was  $\sim 5$  degrees above the western horizon. A series of exposures were made with increasing exposure times, as the background twilight was fading rapidly. The sodium tail of Mercury was easily seen against the twilight and the resonantly scattered sodium light from the Earth's mesosphere. Figure 1d shows an image made from three, 2 minute exposures taken on May 30. A strong gradient in the twilight and terrestrial airglow has been removed so that the image could be contrast stretched to reveal the almost 1.5 degree long tail. The disk of Mercury is hidden behind an occulting mask at the right of the image. At this  $\sim 1$  arc-min/pixel plate scale, the disk of the planet is only  $\sim 0.1$  pixel across. Since Mercury was near greatest eastern elongation at the time the data were taken (and 87 AU from Earth), simple geometry can be used to convert the  $\sim 1.5$  degree angular length of the tail to  $\sim 3.4 \times 10^6$  km or a remarkable  $\sim 1400$  Mercury radii.

[14] Figure 2 is a plot of the peak sodium brightness versus distance down the tail using sliding 3-pixel averages (each  $\sim 15 R_M$  in extent). The data begin beyond the occulting mask that hides Mercury. At several distances, cross-tail brightness patterns are shown using single pixel

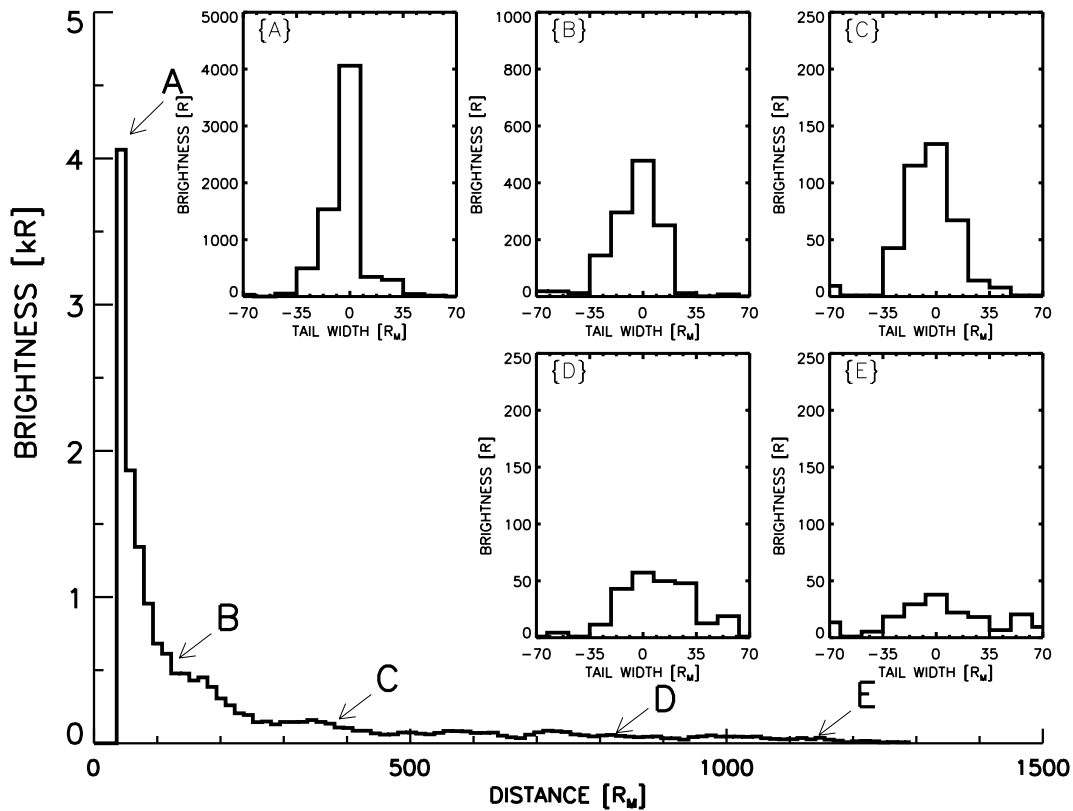


**Figure 2.** A plot of peak sodium brightness above background along the anti-sunward tail direction from the image in Figure 1d. Due to Mercury’s position behind an occulting mask, the data begin at a distance of  $\sim 35 R_M$  from Mercury. (a–e) Cross-tail brightness profiles at the five radial distances indicated.

values. At such distances, the cross tail extent is a fairly uniform  $\pm 35 R_M$ .

### 3. Discussion

[15] As is well known in cometary science, the spatial variability of a tail is determined by episodic changes in gas and dust source rates for neutral tails and/or by temporal changes in the solar wind for plasma tails. Thus, a single picture gives a time-history of the physics acting upon tail gases. For neutral gases escaping a comet nucleus, changes in solar radiation pressure are not an issue since they vary over long time scales (in the absence of a flare); however, a comet’s position and speed in an eccentric orbit do matter. The same is true for Mercury. When interpreting a single image of Mercury’s extensive Na tail, the central issue of relevance is the possibility that source regions might have changed, and thus that tail structures could uncover such variability. For the Moon’s sodium tail, this is indeed the case: meteor showers enhance source rates for a short period of time (few hours in the case of the Leonids). In the 2 days it takes for this enhanced cloud to move in the anti-sunward direction, distinctive signatures in the brightness and orientation of the tail can be observed [Smith *et al.*, 1999]. Such variability patterns serve as robust constraints for modeling the Moon’s neutral Na source rates [Wilson *et al.*, 1999] since the Na photoionization time constant is nearly 2 days. For Mercury, this time constant scales downward as distance squared, and thus becomes  $\sim 7.5$  hours at .4 AU. In the orbital configurations that maximize solar radiation

acceleration at  $\sim 200 \text{ cm/sec}^2$  [Smyth and Marconi, 1995], Mercury’s Na atoms are soon Doppler-shifted out of the Fraunhofer absorption line, essentially to the solar continuum, where they experience a constant acceleration of  $\sim 330 \text{ cm/sec}^2$ .

[16] In 7.5 hours, such Na atoms will move  $\sim 1.2$  million kilometers in the anti-sunward direction, with only 1/e of the atoms ionized. The remaining Na atoms continue to move in the anti-sunward direction to define the tail which, as Figure 1d shows, can be imaged out to  $\sim 3.4$  million km (a distance achieved in less than 2 ionization time constants or  $\sim 14$  hours). Thus, the extraordinary length of the sodium tail portrays Na source conditions versus time. All of the sodium seen in the extended tail was on the surface of Mercury less than a day earlier. The subtle structures seen at  $\sim 300\text{--}400 R_M$  and near  $700 R_M$  might be due to earlier source changes, but they are at the limits of uncertainty.

[17] Ground based observations using the relatively simple technique of wide-angle, low-light-level filtered imaging, when combined with spectrographic techniques for observing sodium close to Mercury, offer a new spatial, and therefore temporal, domain for studies of Mercury’s vast exosphere.

[18] **Acknowledgments.** The observations reported here were made with the cooperation of the director and staff of several observing sites: (a) P. Kervin and colleagues at the AEOS facility on Maui (b) S. Okano, M. Kagitani and students at the Tohoku observatory on Maui, and (c) David Lambert, and the staff of the McDonald Observatory in Texas, host for the Boston University observing station there. Science support came from the joint NSF-AFOSR program for astronomical use of AEOS, from the NASA

Planetary Astronomy and Planetary Atmospheres programs for work at McDonald and Maui, and from the ONR/DURIP program for the image slicer. We thank Boston University graduate student Carl Schmidt for his assistance at the McDonald Observatory during the 2007 IMW campaign and for aiding in the subsequent image data reduction, and Joei Wroten for her help with the initial IMW campaign at AEOS in 2006.

## References

- Barbieri, C., S. Verani, G. Cremonese, A. Sprague, M. Mendillo, R. Cosentino, and D. Hunten (2004), First observations of the Na exosphere of Mercury with the high resolution spectrograph of the 3.5 m Telescopio Nazionale Galileo, *Planet. Space Sci.*, *52*, 1169–1175.
- Baumgardner, J., M. Mendillo, and J. K. Wilson (2000), A digital high-definition imaging system for spectral studies of extended planetary atmospheres. I. Initial results in white light showing features on the hemisphere of Mercury unimaged by Mariner 10, *Astron. J.*, *119*, 2458–2464.
- Chamberlain, J. W., and D. M. Hunten (1987), *Theory of Planetary Atmospheres*, Academic Press, San Diego, Calif.
- Combi, M. R., M. A. DiSanti, and U. Fink (1997), The spatial distribution of gaseous atomic sodium in the comae of comets: Evidence for direct nucleus and extended plasma sources, *Icarus*, *130*, 336–354, doi:10.1006/icar.1997.5832.
- Cremonese, G., et al. (1997), Neutral sodium from comet Hale-Bopp: A third type of tail, *Astrophys. J. Lett.*, *490*, L119.
- Cremonese, G., M. Bruno, V. Mangano, S. Marchi, and A. Milillo (2005), Release of neutral sodium atoms from the surface of Mercury induced by meteoroid impacts (with Corrigendum), *Icarus*, *177*, 122–128.
- Flynn, B., and M. Mendillo (1993), A picture of the Moon's atmosphere, *Science*, *261*, 184–186.
- Huebner, W. F., J. J. Keady, and S. P. Lyon (1992), Solar photo rates for planetary atmospheres and atmospheric pollutants, *Astrophys. Space Sci.*, *195*(1), 1–294.
- Ip, W. H. (1986), The sodium exosphere and magnetosphere of Mercury, *Geophys. Res. Lett.*, *13*, 423–426.
- Kameda, S., M. Kagitani, S. Okano, I. Yoshikawa, and J. Ono (2007), Observations of Mercury's sodium tail using a Fabry-Perot interferometer, *Adv. Space Res.*, in press.
- Killen, R. M., and W.-H. Ip (1999), The surface-bounded atmospheres of Mercury and the Moon, *Rev. Geophys.*, *37*, 361–406.
- Lammer, H., P. Wurz, M. R. Patel, R. Killen, C. Kolb, S. Massetti, S. Orsini, and A. Milillo (2003), The variability of Mercury's exosphere by particle and radiation induced surface release processes, *Icarus*, *166*, 238–247.
- Leblanc, F., and R. E. Johnson (2003), Mercury's sodium exosphere, *Icarus*, *164*, 261–281.
- Leblanc, F., et al. (2006), Observations of Mercury's exosphere: Spatial distributions and variations of its Na component during August 8, 9 and 10, 2003, *Icarus*, *185*, 395–402.
- Leblanc, F., et al. (2007), Mercury's exosphere origins and relations to its magnetosphere and surface, *Planet. Space Sci.*, *55*, 1069–2092, doi:10/1016/j.pass.2006.11.008.
- Mendillo, M., and the IMW team (2007), International Mercury Watch (IMW): Preliminary results of the 2006 Campaign, European Geoscience Union (EGU) meeting, Vienna, *Geophys. Res. Abstr.*, *9*, 05797.
- Mendillo, M., J. Baumgardner, and B. Flynn (1991), Imaging observations of the extended sodium atmosphere of the Moon, *Geophys. Res. Lett.*, *18*, 2097–2100.
- Mierkiewicz, E. J., M. Line, F. L. Roesler, and R. J. Oliverson (2006), Radial velocity observations of the extended lunar sodium tail, *Geophys. Res. Lett.*, *33*, L20106, doi:10.1029/2006GL027650.
- Morgan, T. H., and R. M. Killen (1997), A non-stoichiometric model of the composition of the atmospheres of Mercury and the Moon, *Planet. Space Sci.*, *45*, 81–94.
- Potter, A. E., and T. H. Morgan (1985), Discovery of sodium in the atmosphere of Mercury, *Science*, *229*, 651–653.
- Potter, A. E., and T. H. Morgan (1990), Evidence for magnetospheric effects on the sodium atmosphere of Mercury, *Science*, *248*, 835–838.
- Potter, A. E., and T. H. Morgan (1997), Sodium and potassium atmospheres of Mercury, *Planet. Space Sci.*, *45*, 95–100.
- Potter, A. E., R. M. Killen, and T. H. Morgan (2002), The sodium tail of Mercury, *Meteorit. Planet. Sci.*, *37*, 1165–1172.
- Potter, A. E., R. M. Killen, and M. Sarantos (2006), Spatial distribution of sodium on Mercury, *Icarus*, *181*, 1–12.
- Potter, A. E., R. M. Killen, and T. H. Morgan (2007), Solar radiation acceleration effects on Mercury sodium emission, *Icarus*, *186*, 571–580.
- Smith, S. M., J. K. Wilson, J. Baumgardner, and M. Mendillo (1999), Discovery of the distant lunar sodium tail and its enhancement following the Leonid meteor shower of 1998, *Geophys. Res. Lett.*, *26*, 1649–1652.
- Smith, S. M., M. Mendillo, J. K. Wilson, and J. Baumgardner (2001), Monitoring the Moon's transient atmosphere with an all-sky imager, *Adv. Space Res.*, *27*, 1181–1187.
- Smyth, W. H. (1986), Nature and variability of Mercury's sodium atmosphere, *Nature*, *323*, 696–699.
- Smyth, W. H., and M. L. Marconi (1995), Theoretical overview and modeling of the sodium and potassium atmospheres of Mercury, *Astrophys. J.*, *441*, 839–864.
- Sprague, A. L., et al. (1997), Distribution and abundance of sodium in Mercury's atmosphere, 1985–1988, *Icarus*, *128*, 506–527.
- Sprague, A. L., W. J. Schmitt, and R. E. Hill (1998), Mercury, sodium atmospheric enhancements, radar bright spots, and visible surface features, *Icarus*, *135*, 60–68.
- Stern, S. A. (1999), The lunar atmosphere: History, status, current problems and context, *Rev. Geophys.*, *37*, 453–491.
- Strom, R. G., and A. L. Sprague (2003), *Exploring Mercury: The Iron Planet*, Springer-Praxis, Chichester, U. K.
- Wilson, J. K., J. Baumgardner, and M. Mendillo (1998), Three tails of comet Hale-Bopp, *Geophys. Res. Lett.*, *25*, 225–228.
- Wilson, J. K., S. M. Smith, J. Baumgardner, and M. Mendillo (1999), Modeling an enhancement of the lunar sodium atmosphere and tail during the Leonid meteor shower of 1998, *Geophys. Res. Lett.*, *26*, 1645–1648.
- Wilson, J. K., M. Mendillo, and J. Baumgardner (2005), Io's sodium clouds: A quiet Spring: AAS/DPS Meeting, Cambridge, UK, *Bull. Am. Astron. Soc.*, *37*, 754.

---

J. Baumgardner, M. Mendillo, and J. Wilson, Center for Space Physics, Boston University, Boston, MA 02215, USA. (jeffreymb@bu.edu)